Food & Function

ROYAL SOCIETY OF CHEMISTRY

PAPER

View Article Online
View Journal | View Issue

Check for updates

Cite this: *Food Funct.*, 2026, **17**, 1930

Mechanistic insights into the cholesterol-lowering activity of γ-oryzanol components

Massimiliano Cuccioloni, *[a] Helena Juricic, [a] Laura Bonfili, [a] Ziqi Liu,[b] Giulia Abate,[c] Daniela Uberti,[c] Mauro Angeletti,[a] Anna Maria Eleuteri[a] and Valentina Cecarini[a]

γ-Oryzanol, a mixture of phytosteryl ferulates present in rice bran, has gained attention for its cholesterol-lowering properties, likely due to its interaction with the pharmacological target enzyme 3-hydroxy-3-methyl-glutaryl-coenzyme A reductase (HMGCR). Our study explores the individual contributions of the four major γ-oryzanol constituents, namely cycloartenyl ferulate, campesteryl ferulate, β-sitosteryl ferulate, and 24-methylenecycloartenyl ferulate, to cholesterol synthesis and efflux/excretion. First, according to a concerted approach involving molecular docking, surface plasmon resonance binding studies, and enzyme inhibition assays, we determined the binding affinities and inhibitory activities of each constituent toward HMGCR. Additionally, we evaluated their impact on cholesterol metabolism in HepG2 cells by assessing the cellular cholesterol levels and the expression of selected biomarkers of cholesterol metabolism pathways under non-cytotoxic conditions. The major components of γ-oryzanol, cycloartenyl ferulate (CAF) and 24-methylenecycloartenyl ferulate (24MCAF) significantly affected cholesterol metabolism and reduced cellular cholesterol levels *via* distinct mechanisms, despite their highly conserved chemical structures. Specifically, CAF reduced the total and free cholesterol levels, consequently triggering a compensatory activation of the SREBP-2 pathway, marked by increased HMGCR and LDL receptor expression, whereas 24MCAF moderately lowered cholesterol and enhanced its clearance primarily by upregulating the cholesterol efflux transporter ABCG1. Instead, both CAF and 24MCAF comparably affected ABCA1, another cholesterol efflux regulatory protein, and CYP7A1, essential for converting cholesterol into bile acids. Together, these dynamics reveal a dual modulation that supports the lipid-lowering effects of γ-oryzanol components and highlights their potential as therapeutic agents in cholesterol management.

Received 10th August 2025,
Accepted 15th January 2026

DOI: 10.1039/d5fo03394b

rsc.li/food-function

Open Access Article. Published on 21 January 2026. Downloaded on 3/3/2026 10:07:28 AM.
This article is licensed under a Creative Commons Attribution 3.0 Unported Licence.

Introduction

Cardiovascular diseases are the leading cause of death worldwide,[1] with hypercholesterolemia being recognized as a modifiable risk factor for atherosclerosis and coronary heart diseases.[2] Statins, potent inhibitors of 3-hydroxy-3-methyl-glutaryl-coenzyme A reductase (HMGCR), the rate-limiting enzyme in cholesterol biosynthesis, are among the most widely prescribed treatments for hypercholesterolemia because of their ability to lower circulating cholesterol levels.[3] However, statin therapy is often limited by adverse effects such as muscle pain, liver enzyme alterations, and increased risk of type 2 diabetes, which can reduce patient compliance and underscore the need for safer alternative treatments.[4,5] In this context, natural bioactive compounds have emerged as promising candidates owing to their cholesterol-lowering effects coupled with potentially improved safety profiles.[6,7] Among these, γ-oryzanol, a mixture of phytosteryl ferulates derived from rice bran oil,[8] has attracted great interest for its documented cholesterol-lowering properties,[9] possibly mediated by HMGCR inhibition.[10] Several extraction methods, including solvent extraction, ultrasonic-assisted extraction, and supercritical CO_2 extraction, have been developed, each yielding adequate-quality γ-oryzanol fractions with preserved bioactivity suitable for functional studies.[11–15] The four major components of γ-oryzanol are cycloartenyl ferulate (CAF), 24-methylenecycloartenyl ferulate (24MCAF), β-sitosteryl ferulate (SF), and campesteryl ferulate (CampF), known for their antioxidant and anti-inflammatory properties,[16–18] which likely contribute to lipid metabolism regulation.[19,20] Although the cholesterol-lowering effects of whole γ-oryzanol mixtures have been demonstrated, the precise contributions of individual constituents to HMGCR inhibition and cellular cholesterol

[a]*School of Biosciences and Veterinary Medicine, University of Camerino, via Madonna delle Carceri, 62032 Camerino, MC, Italy.*
E-mail: massimiliano.cuccioloni@unicam.it
[b]*College of Food Science and Engineering, Jilin Agricultural University, Jilin, 130118, China*
[c]*Department of Molecular and Translational Medicine, University of Brescia, Italy*

This journal is © The Royal Society of Chemistry 2026

Open Access Article. Published on 21 January 2026. Downloaded on 3/3/2026 10:07:28 AM.
This article is licensed under a Creative Commons Attribution 3.0 Unported Licence.

synthesis and excretion remain to be elucidated.[21,22] Hepatic cholesterol homeostasis is maintained through an integrated network balancing cholesterol biosynthesis, uptake, efflux, and catabolism.[23] Central to this regulation is sterol regulatory element-binding protein 2 (SREBP-2), a transcription factor that responds to intracellular cholesterol depletion by promoting the expression of genes critical for cholesterol metabolism, including HMGCR and the low-density lipoprotein receptor (LDLR), which mediates cholesterol uptake.[24,25] Complementing SREBP-2-driven biosynthesis and uptake, liver X receptors (LXRα/β) act as cholesterol sensors that are activated by oxysterols and limit cholesterol accumulation by upregulating ATP-binding cassette transporters ABCA1 and ABCG1, thereby enhancing cholesterol efflux to extracellular acceptors and supporting reverse cholesterol transport.[25] Our work aims to elucidate the distinct and complementary mechanisms by which γ-oryzanol major components modulate cholesterol synthesis and efflux/excretion pathways, and highlight their potential as natural alternatives or adjuncts to statins. Specifically, we integrated a multidisciplinary approach combining molecular docking, surface plasmon resonance binding assays, enzymatic activity evaluations, and cellular assays in HepG2 cells to characterize the interactions and functional effects of individual γ-oryzanol constituents. Globally, we assessed the inhibitory potency of CAF and 24MCAF (the most abundant constituents of γ-oryzanol) against HMGCR, which affected cholesterol levels and the expression of key biomarkers (SREBP-2, LXRα/β, HMGCR, LDLR, ABCA1, ABCG1, and CYP7A1), providing mechanistic insights into their distinct roles in cholesterol synthesis and excretion. Our results support their potential as natural agents for cholesterol management and as alternatives or adjuncts to statin therapy.

Results and discussion

Characterization of rice bran extract

Pressurized liquid extraction of rice bran was efficiently accomplished using an ASE 100 system under the conditions described in the Experimental section. The crude extract was separated by RP-HLPLC to resolve its constituent fractions. Resulting chromatograms revealed a distinct biphasic elution pattern.

An initial polar fraction was eluted rapidly from the column, with a retention volume of approximately 1.8 mL. Next, the chromatogram revealed a later apolar fraction, manifesting as four well-defined peaks at retention volumes of 6.2, 6.95, 7.3, and 8.3 mL (Fig. 1). The comparison with a commercial γ-oryzanol standard confirmed this latter fraction as enriched in γ-oryzanol-related components, and MS analysis unambiguously identified these four peaks as CAF, 24MCAF, SF, and CampF (Table S1).

Molecular docking

To evaluate the potential statin-like properties of the molecules of interest, a preliminary molecular docking study was performed to characterize the interaction between the major γ-oryzanol constituents and the catalytic domain of human HMGCR. Each ligand was independently docked onto the HMGCR crystal structure, and the resulting binding conformations were comprehensively analyzed. Consistent with analogous studies,[26] the four γ-oryzanol components exhibited a highly conserved binding mode within the HMGCR catalytic pocket, stabilized by H-bonds, hydrophobic and polar interactions, as shown in Fig. 2 (left and right panels). Binding interface mapping identified a set of amino acid residues (AA 521–525) recurrently involved in stabilizing the binding of all four molecules (Table S2), underscoring the shared molecular recognition motif. The superposition of the docked complexes further showed analogous accommodation of the steryl ferulate moieties, facilitating direct interactions with amino acids close to the catalytic tetrad (Lys691, Glu559, Asp767, and His866[27]), most likely hindering the active site accessibility.

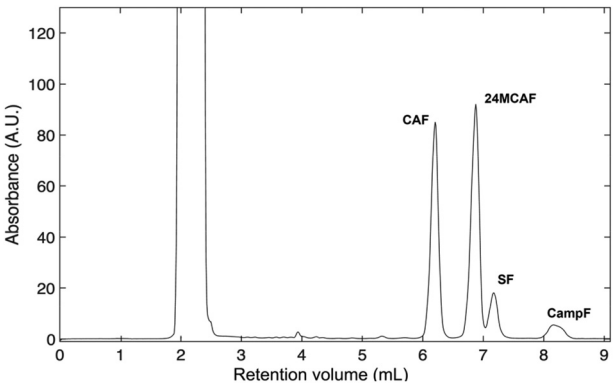

Fig. 1 HPLC profile of elution of the rice bran hydroalcoholic extract.

Predicted binding free energies (ΔG) indicated moderately-high and comparable complex stability for each γ-oryzanol constituent, with values from −7.463 to −7.871 kcal mol^{-1}, reflecting favourable thermodynamics. Dissection of binding energies revealed similar energetic contributions (intermolecular contacts, van der Waals, and electrostatic interactions) for all ligands, supporting a common binding mechanism and suggesting analogous modulatory effects on the HMGCR activity (Table 1).

Binding of γ-oryzanol components to HMGCR

To experimentally prove the data obtained from the computational analysis, the molecular interactions between CAF, 24MCAF, SF, CampF and HMGCR were evaluated using a biosensor-based approach. In line with molecular docking, all four γ-oryzanol constituents demonstrated reversible binding to surface-immobilized HMGCR, as evidenced by the baseline recovery upon multiple PBS buffer washes. The mono-exponential kinetic profiles observed for each interaction suggest the presence of a single high-affinity binding site on HMGCR for these phytochemicals, supporting a 1 : 1 binding stoichiometry (Fig. 3). Among the tested compounds, CAF was the best binder, being characterized by the highest association rate

Open Access Article. Published on 21 January 2026. Downloaded on 3/3/2026 10:07:28 AM.
This article is licensed under a Creative Commons Attribution 3.0 Unported Licence.

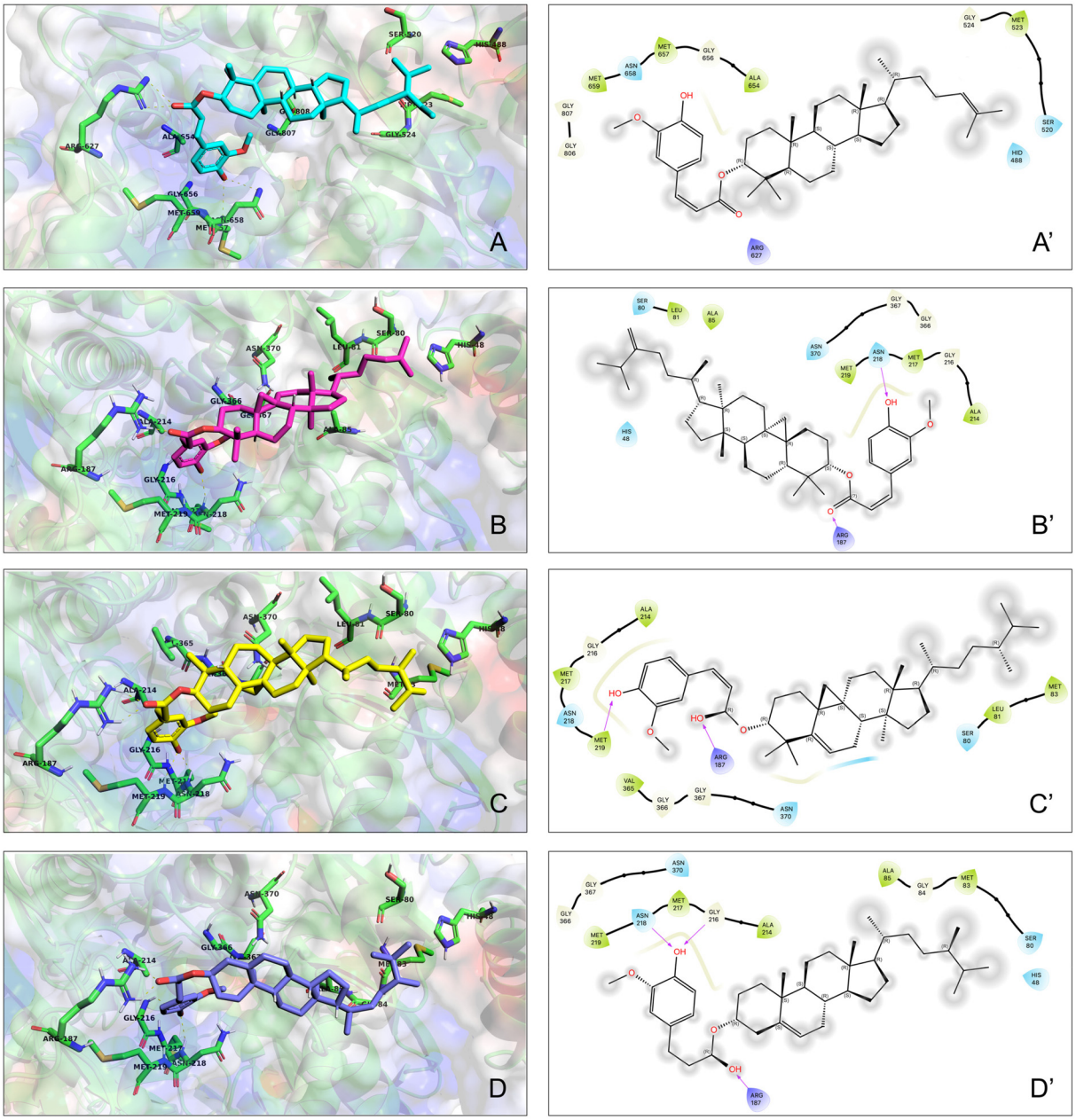

Fig. 2 3D docking models of the four main components of γ-oryzanol binding to HMGCR (left panels), and 2D details of the interactions with the AA in proximity to the catalytic site (right panels). H-bonds are shown as purple arrows; hydrophobic interactions are shown as green ribbon; polar interaction are shown as light blue ribbon; fading grey circles identify solvent-exposed atoms; boxes A and A′: cycloartenyl ferulate (CAF); boxes B and B′: 24-methylene-cycloartenyl ferulate (24MCAF); boxes C and C′: β-sitosteryl ferulate (SF); boxes D and D′: campesteryl ferulate (CampF).

constant and the lowest dissociation rate constant. This kinetic signature indicates that CAF forms the most stable complex with HMGCR, resulting in the highest binding affinity. Conversely, 24MCAF, SF, and CampF displayed lower and comparable affinities, with only minor differences in their kinetic parameters (Table 2).

HMGCR inhibition

Once the ability of the γ-oryzanol components to bind HMGCR in a region likely overlapping to its catalytic domain was established, the individual inhibitory effects of CAF, 24MCAF, SF, and CampF toward HMGCR activity were systematically evaluated using a spectrophotometric assay based on monitoring the changes in the NADPH absorbance upon incubation with different concentrations of the molecules of interest. All four components demonstrated potent inhibition of HMGCR, with IC_{50} values in the submicromolar range (Table 3). Among these, 24MCAF exhibited the highest potency (IC_{50} = 0.04 μM), followed by CAF, with SF and CampF showing similar but slightly lower inhibitory activities.

This journal is © The Royal Society of Chemistry 2026

Open Access Article. Published on 21 January 2026. Downloaded on 3/3/2026 10:07:28 AM. This article is licensed under a Creative Commons Attribution 3.0 Unported Licence.

Table 1 Predicted affinities and energy contribution values for the complexes formed between the human HMGCR and the four major γ-oryzanol constituents. Total internal energy term consists of torsional energy and repulsion at short distances, van der Waals and electrostatic contributions

Compound	Score (kcal mol^{-1})	Intermol. energy (kcal mol^{-1})	vdw energy (kcal mol^{-1})	Electr. energy (kcal mol^{-1})
CAF	−7.463	−35.933	−11.755	−24.178
24MCAF	−7.661	−37.835	−13.419	−24.416
SF	−7.871	−41.160	−13.301	−27.859
CampF	−7.557	−39.988	−12.372	−27.616

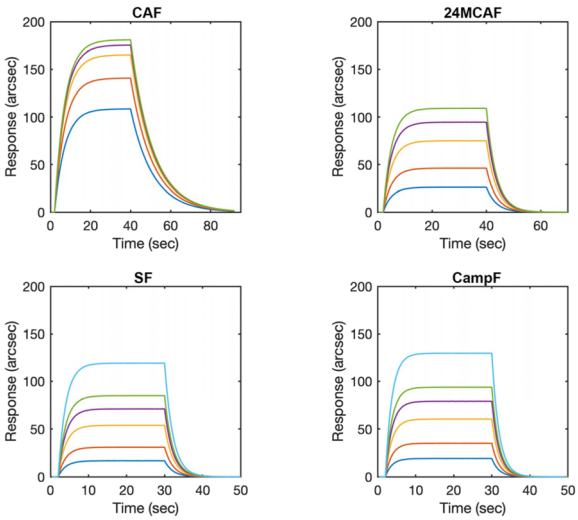

Fig. 3 Representative sensorgrams obtained upon interaction of the individual soluble γ-oryzanol components with surface-blocked human HMGCR.

Table 2 Kinetic and equilibrium parameters of the complexes between HMGCR and oryzanol constituents

Molecule	k_{ass} (M^{-1} s^{-1})	k_{diss} (s^{-1})	K_D (μM)
CAF	41046 ± 5377	0.01 ± 0.007	0.23 ± 0.16
24MCAF	16151 ± 4731	0.03 ± 0.006	1.76 ± 0.62
SF	16233 ± 5081	0.05 ± 0.006	2.83 ± 0.97
CampF	20551 ± 3576	0.05 ± 0.007	2.58 ± 0.58

Table 3 Individual inhibitory potency of the major γ-oryzanol components

Molecule	IC_{50} (μM)
CAF	0.46 ± 0.02
24MCAF	0.04 ± 0.02
SF	0.50 ± 0.01
CampF	0.10 ± 0.01

Kinetic analysis revealed that 24MCAF, SF, and CampF act as competitive inhibitors of HMGCR, as indicated by residual activity plots (Fig. 4), whereas CAF displayed an allosteric

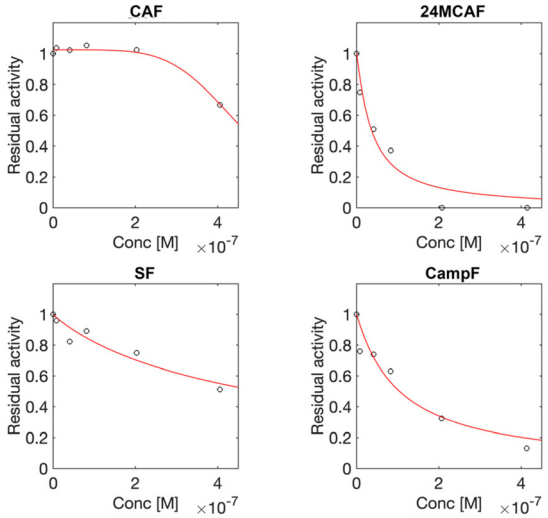

Fig. 4 Effect of the individual major γ-oryzanol components on the enzymatic residual activity of HMGCR.

mode of inhibition.[28] These findings highlight the strong and diverse inhibitory mechanisms of the γ-oryzanol components against HMGCR, supporting their potential contribution to the cholesterol-lowering effects observed for γ-oryzanol.[21,22]

Effects of treatments on cholesterol levels

CAF and 24MCAF (the major components of γ-oryzanol) were selected for the evaluation of their cholesterol-lowering efficacy in a hepatic cell model.

The total and free cholesterol (TC and FC, respectively) in HepG2 cells after 24 h treatments were measured with the AmplexRed Cholesterol assay kit. TC and FC cholesterol decreased upon treatments, showing a similar behaviour (Fig. 5). The decrease was mainly evident upon exposure to γ-oryzanol (ORY) and CAF. An even lower significant reduction in cholesterol levels was observed upon 24MCAF treatment (approximately 15% decrease compared to that in the control). Moreover, CAF and 24MCAF showed a non-additive cholesterol-lowering effect when combined at total concentrations equal to the sum of individual treatments. In fact, CAF (a weaker but high-affinity allosteric HMGCR binder) likely saturated the enzyme's allosteric site, limiting 24MCAF's access to the active site. Cellular feedback mechanisms could further buffer cholesterol reduction, explaining why 24MCAF's stronger inhibitory capacity does not enhance the combined effect.[29–31]

Treatments activate the SREBP-2 signaling pathway

Beside the direct HMGCR inhibition, to further elucidate the mechanisms underlying the reduced cholesterol levels observed following treatment with γ-oryzanol, CAF, and 24MCAF, we assessed the expression of markers of the SREBP-2 (sterol regulatory element-binding protein 2) signaling pathway, specifically, SREBP-2, HMGCR and LDL receptor (LDLR). SREBP-2 is a key transcription factor central to chole-

Open Access Article. Published on 21 January 2026. Downloaded on 3/3/2026 10:07:28 AM.
This article is licensed under a Creative Commons Attribution 3.0 Unported Licence.

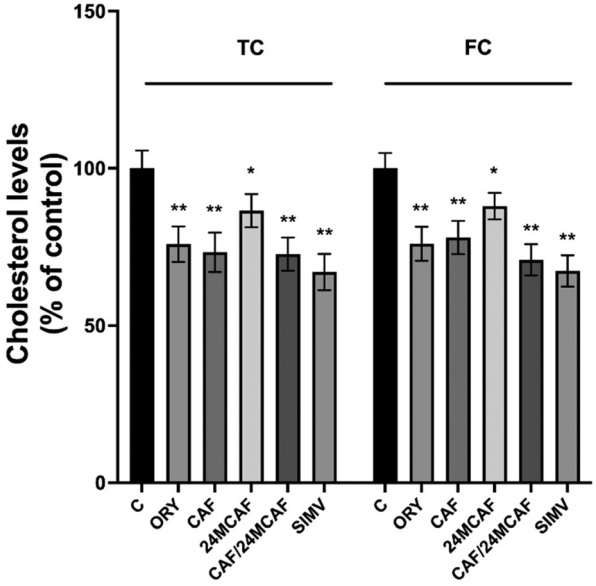

Fig. 5 Levels of TC and FC upon γ-oryzanol, CAF, 24MCAF (individual and combined) and simvastatin treatment. HepG2 cells were treated as described in the Experimental section. TC and FC levels were measured following the kit protocols. Asterisks indicate data points statistically significant with respect to the control (*$p < 0.05$ and **$p < 0.01$).

sterol homeostasis. Upon cleavage, occurring under low cholesterol conditions, its mature form enters the nucleus to activate the transcription of target genes including LDLR and HMGCR, thereby upregulating cholesterol uptake and synthesis to maintain cholesterol homeostasis.[24] Notably, we observed an increase in the expression of both the precursor and mature forms of SREBP-2, with the ratio mature/precursor SREBP-2 elevated after treatments, suggesting the activation of the SREBP-2 pathway and the enhanced proteolytic processing of this transcription factor. Additionally, all treatments, mainly CAF, significantly increased the expression levels of both HMGCR and LDLR (Fig. 6), further confirming the upregulation of this signaling pathway. This activation likely reflects a compensatory cellular response aimed at restoring cholesterol homeostasis in the context of cholesterol depletion.[32,33] Collectively, these findings indicate that in HepG2 cells, γ-oryzanol, CAF, and 24MCAF activate the SREBP-2 pathway as part of a feedback regulatory loop, a mechanism comparable to that triggered by simvastatin,[34] although with a lower potency.

Treatment enhances cholesterol efflux and catabolism markers

In line with the hypothesized complementary mechanisms by which γ-oryzanol components modulate cholesterol synthesis and excretion, treatment of HepG2 cells with γ-oryzanol and its isolated major components (CAF and 24MCAF) resulted in a significant upregulation of key genes involved in cholesterol efflux and metabolism. ABCA1 and ABCG1 genes encode ATP-binding cassette transporters that mediate cholesterol efflux to apolipoproteins and high-density lipoprotein (HDL), thereby facilitating reverse cholesterol transport and reducing intra-

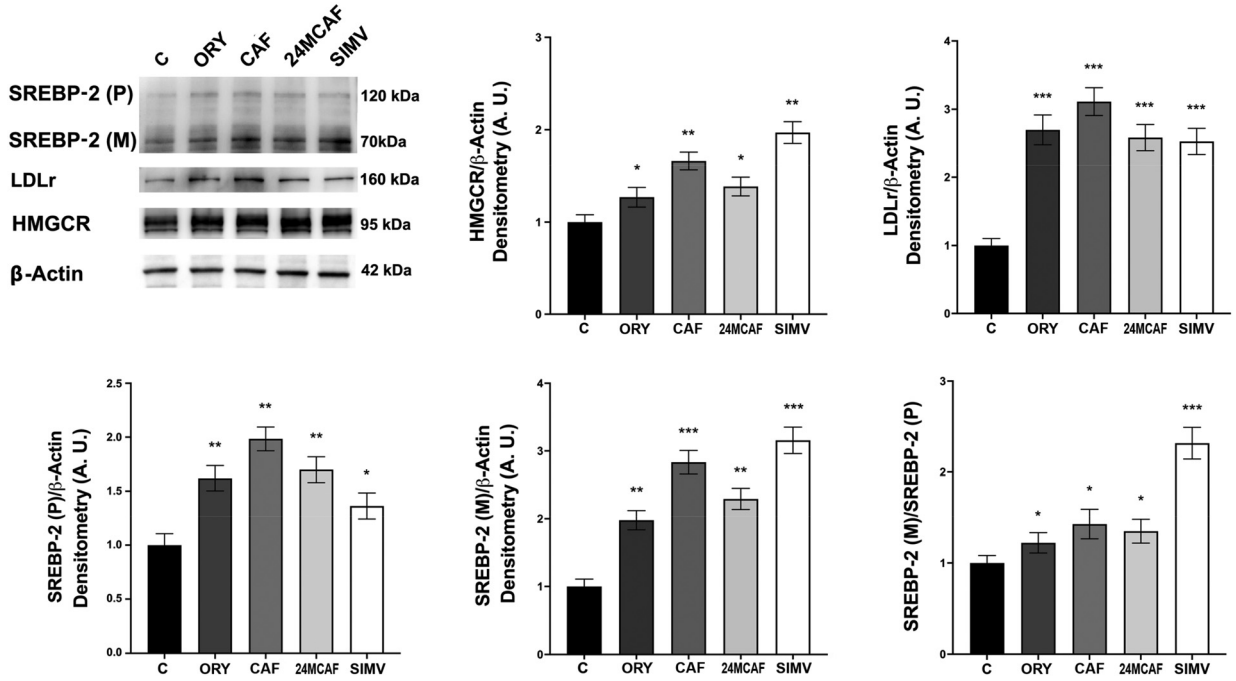

Fig. 6 Effects of treatments on the SREBP-2 signalling pathway. SREBP-2, LDLr and HMGCR expression levels detected in HepG2 cells treated for 24 h with ORY, CAF, 24MCAF and simvastatin. The ratio SREBP-2 (M)/SREBP-2 (P) is also indicated. Equal protein loading was verified by using an anti-β-actin antibody and normalized expressions are reported as arbitrary units (A.U.). Experiments were performed in triplicate. Asterisks indicate data points statistically significant with respect to the control (*$p < 0.05$, **$p < 0.01$, and ***$p < 0.001$).

This journal is © The Royal Society of Chemistry 2026

Open Access Article. Published on 21 January 2026. Downloaded on 3/3/2026 10:07:28 AM.
This article is licensed under a Creative Commons Attribution 3.0 Unported Licence.

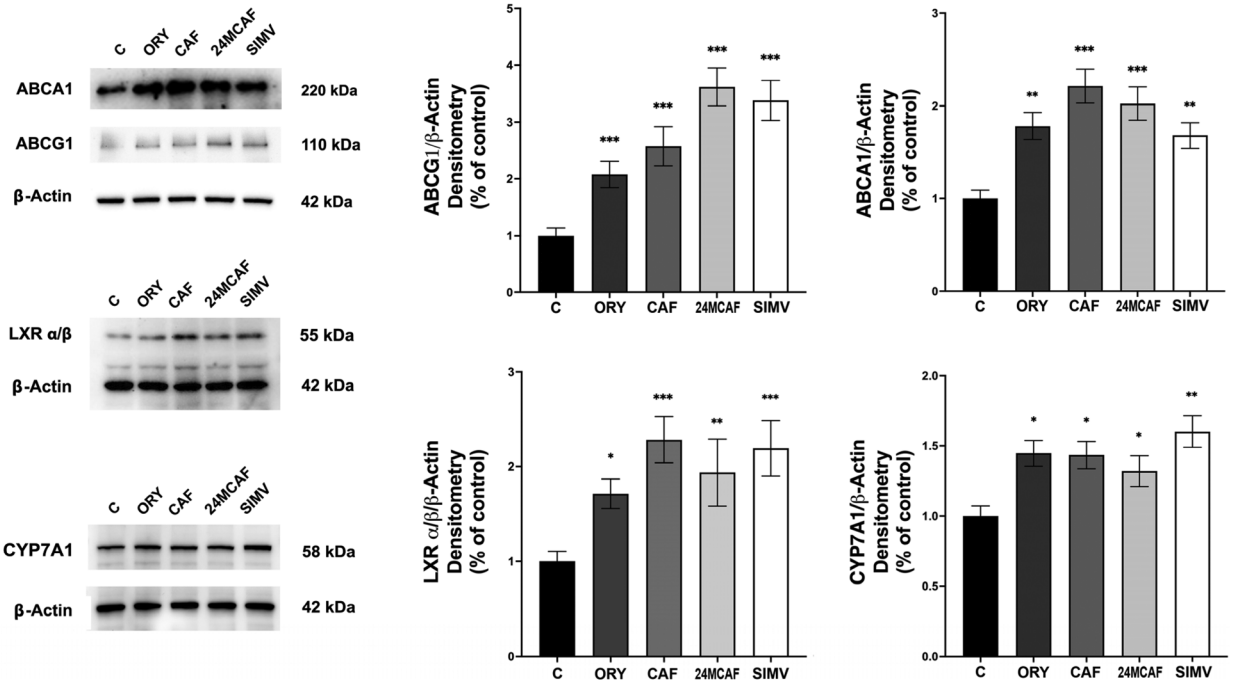

Fig. 7 Effects of treatments on ABCA1, ABCG1, LXRα/β and CYP7A1 proteins. ABCA1, ABCG1, LXRα/β and CYP7A1 expression levels were detected using specific primary antibodies. Equal protein loading was verified by using an anti-β-actin antibody and normalized expressions are reported as arbitrary units (A.U.). Experiments were performed in triplicate. Asterisks indicate data points statistically significant with respect to the control (*p < 0.05, **p < 0.01, and ***p < 0.001).

cellular cholesterol accumulation.[25] All treatments increased the expression of both transporters, with 24MCAF inducing the most pronounced effect on ABCG1, resulting in a 3.6-fold increase compared to the control, an effect comparable to that of simvastatin (Fig. 7). Both CAF and 24MCAF treatments elicited a 2.0-fold increase in ABCA1 expression. CYP7A1, cholesterol 7α-hydroxylase, the rate-limiting enzyme in bile acid synthesis, was significantly upregulated in response to treatments, indicating enhanced cholesterol catabolism. Most notably, these findings align with the compensatory activation of the SREBP2 pathway observed under treatment conditions and demonstrate that γ-oryzanol and its major components simultaneously promote mechanisms that decrease intracellular cholesterol *via* increased efflux and catabolism.

Experimental

Materials

γ-Oryzanol, Na_2HPO_4, CH_3COONa, KCl, NaCl, Tween-20, EDTA, DTT, DMSO, HMG-CoA, human HMGCR, NADPH, simvastatin, CH_3OH, C_2H_5OH, and CH_3CN were all obtained from Merck-Sigma (Milan, Italy). HepG2 cells (HB-8065) were obtained from ATCC. All chemicals were of the highest grade available. Media, reagents and plastics for cell cultures were purchased from Corning (Tewksbury, MA, USA). Rice bran sample ("Volta" rice variety) was kindly provided by Società Italiana Sementi (Bologna, Italy). Cycloartenyl ferulate (CAF) and 24-methylene-cycloartenyl ferulate (24MCAF), β-sitosteryl ferulate (SF), and campesteryl ferulate (CampF) were obtained from ChemFaces (Wuhan, Hubei – China). 3-(4,5-Dimethyl-2-thiazolyl)-2,5-diphenyl-2*H*-tetrazolium bromide (MTT) used in cytotoxicity assays was obtained from Merck Spa (Milan, Italy). Membranes for western blot analyses were purchased from Biorad (Milan, Italy). Immunodectection was performed with Clarity Western ECL substrates (Biorad, Milan, Italy). Precast gels used for SDS-PAGE were from Biorad, Milan, Italy. Binding studies were performed on an IAsys *plus* biosensor obtained from Thermo Fisher Scientific (Milan, Italy). Carboxymethyl-dextran (CMD) cuvettes, 1-ethyl-3-(3-dimethylaminopropyl)-carbodiimide (EDC), *N*-hydroxysuccinimide (NHS), and ethanolamine were obtained from Farfield Group (Cheshire, UK). The Cary 100 Bio UV-vis spectrophotometer was obtained from Varian (Palo Alto, CA). The AKTA Basic 10 HPLC system with a UV-vis detector and HPLC column heater were obtained from Amersham. (Milan, Italy). A Kinetex 5 μm EVO C18 150 × 4.6 mm column, equipped with a 5 mm guard column was purchased from Phenomenex Italia (Bologna, Italy). Fluorescence data were acquired on a SpectraMax Gemini XPS microplate reader (Molecular Device, Milan, Italy).

Accelerated solvent extraction of γ-oryzanol

Bran samples were stored in a cool, dry environment prior to processing. A Dionex ASE 100 accelerated solvent extractor (Dionex Corporation, Sunnyvale, CA) equipped with 100 mL stainless extraction cells and 250 mL glass collection bottles

Open Access Article. Published on 21 January 2026. Downloaded on 3/3/2026 10:07:28 AM.
This article is licensed under a Creative Commons Attribution 3.0 Unported Licence.

with Teflon-coated rubber caps was used for the extraction of γ-oryzanol from rice bran, as previously described by Echenique and colleagues,[35] with some modifications. The cell was filled with 10 g of rice bran. Extraction parameters were T = 100 °C, pressure = 1500 psi, pre-heating period = 5 min, static extraction period = 5 min, solvent flash = 9.9 mL, and nitrogen purge = 60 s. A solution of ethanol/water (80 : 20) was used as the extraction solvent, and both static extraction and solvent flash were performed twice *per* sample. Following extraction, the solution (100 mL) was concentrated to dryness using a Büchi rotary evaporator under reduced pressure; the resulting residue was subsequently stored at −20 °C in sealed bottles protected from light until further use.

Isolation of γ-oryzanol components

Rice bran extracts were characterized using an AKTA Basic 10 HPLC system, essentially as described by Abate and colleagues,[36] with some minor modifications. Briefly, the dry extract was resuspended in methanol, ultrasonicated at 37 °C and 37 kHz for 15 min on an Elmasonic Select device (Elma), filtered with 0.2 μm cellulose acetate syringe filters (Scharlab S.L. – Barcelona, Spain), and separated by RP-HPLC with a Kinetex EVO C18 column with an isocratic mobile phase consisting of methanol and acetonitrile (40 : 60 v/v ratio), flow rate of 0.6 mL min^{-1}, 10 μL of injection volume, and analysis temperature of 37 °C. Detection was performed at 280 and 323 nm. γ-Oryzanol constituents were identified by mass spectrometry (MS) analysis based on the comparison with reference standards using an LCQ Fleet Ion Trap MS^n electrospray ionization spectrometer (Thermo Fisher Scientific, Waltham, MA, USA) in negative ionization mode (m/z 100–2000). ESI parameters were set as follows: source voltage of 5.3 kV, capillary voltage of −16.00 V, capillary temperature of 350 °C, and nitrogen sheath (35 arb) and auxiliary (15 arb) gas. Data analysis was conducted using Xcalibur software 4.0.27.13 (Thermo Fisher Scientific, Waltham, MA, USA). Upon identification, individual major constituents were collected, freeze-dried on a CentriVap centrifugal concentrator (LabConco, Fort Scott, KS), and stored at −20 °C until use. Purity (>98%) was assessed in compliance to Papadoyannis and colleagues, by comparing individual absorbance spectra at different wavelengths to confirm peak homogeneity and exclude impurities.[37]

Molecular docking

The most probable binding models between the four major constituents of γ-oryzanol and HMGCR were determined by molecular docking using AutoDock 4.2, which employs a Lamarckian genetic algorithm and semi-empirical free energy force field to explore ligand binding possibilities to explore the binding possibilities of a ligand in a binding pocket.[38] The X-ray crystal structure of human HMGCR (pdb entry: 3CCT[39]) was obtained from the RCSB Protein Data Bank.[40] Protein preparation included removal of water molecules, addition of polar hydrogens, and assignment of Gasteiger partial charges. The resulting receptor structure was saved in PDBQT format. The molecules of interest were retrieved from Pubchem,[41] energy minimized and prepared for docking with Avogadro2 Ver.1.100.0 using the MMFF94 force field.[42] Hydrogens were added, structures were geometry optimized, and then converted to PDBQT format in AutoDockTools. Docking analysis was performed as previously reported,[43] with a grid of 50 × 50 × 50 points around the catalytic pocket of HMGCR; grid spacing: 0.375 Å; rms tolerance: 0.8 Å; maximum energy evaluations: 2 500 000; unless stated differently, all parameters were set to default values. Multiple independent docking runs per ligand were executed, and the resultant conformations were clustered and ranked for binding energy and cluster population. The complexes with the lowest binding energy (kcal mol^{-1}) and root mean square deviation (RMSD) of less than 1.5 Å were selected as the best docking pose. 3D models were rendered with PyMOL (The PyMOL Molecular Graphics System, Version 3.0.3 Schrödinger, LLC), and 2D models were rendered with Maestro (Schrödinger Release 2025-3: Maestro, Schrödinger, LLC, New York, NY, 2025).

Binding to HMGCR

The interaction between each major γ-oryzanol components and HMGCR was explored, according to a biosensor-based approach. Briefly, the CMD-surface of the IAsys *plus* biosensor was activated with a 50 mM equimolar mixture of EDC/NHS,[44] then functionalized with a 100 μg mL^{-1} solution of human HMGCR dissolved in CH_3COONa (10 mM). Finally, any remaining activated carboxylic groups that were still available were blocked with 1 M ethanolamine (pH 8). Upon immobilization, the preservation of the native-like conformation and functionality of the enzyme were assessed by independently checking the interaction with HMG-CoA and NADPH, as previously reported.[45] Then, surface-blocked HMGCR was tested for binding to the compounds of interest at different concentrations in the range of 0.2–3 μM, each time assessing the baseline recovery between the independent bindings. Ligand dissociation and HMGCR baseline recovery were performed with repeated PBS washes. The biosensor chamber was set at 37 °C throughout the experiment. Raw data were analysed with mono- and bi-exponential models using Fast Fit software (Fison Applied Sensor Technology; Affinity Sensors), with the validity of each model to the fit time courses being established by the F-test procedure.

HMGCR inhibition

The effect of the γ-oryzanol components of interest on the activity of HMGCR was evaluated by monitoring the decrease in the NADPH absorbance at 340 nm, which corresponds to NADPH oxidation during the catalytic conversion of HMG-CoA to mevalonate.[46] Briefly, HMGCR (4 nM) was individually incubated under continuous gentle stirring for 20 min at 37 °C with increasing concentrations of each γ-oryzanol component in the range of 0–0.4 mM in the activity buffer (100 mM phosphate buffer containing 1 mM EDTA, 10 mM DTT, and 2% DMSO, pH 6.8). The HMGCR enzymatic activity was continuously monitored after the addition of both free and ligand-pre-incubated enzyme to assay mixtures containing NADPH and

 This journal is © The Royal Society of Chemistry 2026

Open Access Article. Published on 21 January 2026. Downloaded on 3/3/2026 10:07:28 AM. This article is licensed under a Creative Commons Attribution 3.0 Unported Licence.

HMG-CoA (50 mM each). Residual activities were measured at 340 nm on a Cary 100 Bio UV-Vis spectrophotometer (Varian) by continuously monitoring the NADPH absorbance after the initiation of the reaction. The residual activity was expressed as the ratio of the slopes corresponding to the linear decrease in NADPH absorbance with time (2 min) in the presence and in the absence of a given ligand concentration. Raw data were eventually analysed with a standard model for enzyme inhibition, as previously reported.[6]

Cell treatment and viability assay

HepG2 cells were grown in DMEM supplemented with 10% foetal bovine serum (FBS), 2 mM L-glutamine, 1 mM sodium pyruvate, 1% antibiotic and antimycotic, at 37 °C with 95% air and 5% CO_2. Cell viability was evaluated with the MTT assay. In detail, after 24 h exposure to increasing concentrations of γ-oryzanol, CAF and 24MCAF, cells were washed in PBS (pH 7.5), exposed to MTT dissolved in medium without FBS (final concentration, 0.5 mg mL^{-1}) and incubated at 37 °C for 2 h. Then, the medium was replaced with DMSO (100 μL). Control cells were treated with DMSO. Three independent experiments, each with six replicates, were performed. The optical density was measured at 550 nm in a microtiter plate reader. For cholesterol measurements and western blotting assays, cells were plated on 6-well plates and exposed to γ-oryzanol (10 μg mL^{-1}, the highest non-cytotoxic concentration achievable without causing precipitation), CAF (6.7 μg mL^{-1} ≈ 11 μM), 24MCAF (8 μg mL^{-1} ≈ 13 μM) and simvastatin (40 μM) for 24 h, with the individual concentrations being selected based on the results of the cytotoxicity studies (Fig. S1). Experiments were performed in triplicate. After 24 h, the medium was removed, cells were washed with PBS, collected with a scraper in RIPA lysis buffer and transferred in ice for 30 min with intermittent vortexing. Then, cells were centrifuged at 13 000*g* for 10 min. Supernatants were stored at −80 °C until use and the protein concentration was measured by the Bradford assay using bovine serum albumin as the standard.[47]

Cholesterol levels

Total (TC) and free cholesterol (FC) in HepG2 cells treated with γ-oryzanol, CAF, 24MCAF and simvastatin were quantified with the AmplexRed Cholesterol assay kit (Waltham, MA, USA) with values normalized to the total cellular protein quantified *via* Bradford assay. The TC content was determined by measuring the cholesterol concentration in the presence of the enzyme cholesterol esterase. To measure FC, cholesterol esterase was omitted from the assay. Upon treatments, cells were collected in RIPA lysis buffer as abovementioned. The working solution was freshly prepared in reaction buffer, according to the datasheet, and contained Amplex® Red reagent (300 μM), horseradish peroxidase (2 U mL^{-1}), cholesterol oxidase (2 U mL^{-1}), and cholesterol esterase (0.2 U mL^{-1}). A cholesterol standard curve was created by diluting the provided cholesterol reference standard (5.17 mM) in reaction buffer. A 50 μL volume of cell lysates diluted by 1 : 10 in reaction buffer and 50 μL of the working solution were placed on a 96-well plate and incubated at 37 °C. Fluorescence measurements were recorded after 30 min on a SpectraMax Gemini XPS microplate reader (λ_{exc} = 540 nm, λ_{em} = 590 nm). Each sample was set up in triplicate within the assay, and three independent experiments were performed.

Protein biomarkers of cholesterol synthesis and excretion

Proteins were resolved by SDS–PAGE (8%–12% acrylamide) and then transferred onto PVDF membranes. Membranes were incubated with primary monoclonal antibodies to detect HMGCR (Antibodies.com, Stockholm, Sweden), SREBP-2, LDLR, ABCA1, CYP7A1 (Santa Cruz Biotechnology, Heidelberg, Germany) and ABCG1 (Thermo Fisher Scientific, Italy) proteins, and then with the specific peroxidase-conjugated secondary antibodies. ECL western blotting detection reagents were used to detect proteins at the ChemiDoc MP system. Molecular weight markers (10–250 kDa, Biorad, Milan, Italy) were loaded in each gel. Membranes were stripped and reprobed with an anti-β-Actin (Santa Cruz Biotechnology, Heidelberg, Germany) monoclonal antibody to ensure for equal protein loading. The stripping buffer contained 200 mM glycine, 0.1% SDS, and 1% Tween 20. Protein bands were quantified using ImageJ 1.52a software (NIH, Bethesda, MD, USA) and normalized to β-actin.

Statistical analysis

Data are presented as mean values with standard deviations. Statistical analysis was performed with one-way ANOVA, followed by the Bonferroni *post hoc* test using GraphPad Prism software version 10.2.1, and a *p*-value less than 0.05 was considered statistically significant.

Conclusions

This study provides a comprehensive analysis of the individual effects of the two major γ-oryzanol constituents on cholesterol synthesis and excretion. Through an integrative approach combining molecular docking, SPR binding assays, enzymatic inhibition, and cellular cholesterol quantification in HepG2 cells, we have elucidated their distinct molecular interactions and functional impacts. Molecular docking and SPR analyses revealed that all constituents engage a conserved binding mode within the catalytic pocket of HMGCR, with CAF exhibiting the highest binding affinity (K_D ≈ 0.23 μM) due to its stable enzyme interaction. However, it is important to acknowledge that docking studies inherently capture static interactions focused on the active site, and may not fully reflect dynamic enzyme conformational changes or alternative binding modes. Consistent with this, experimental kinetic analyses demonstrate that CAF functions as an allosteric inhibitor, suggesting it may also bind to distinct regulatory sites on HMGCR, modulating enzyme activity indirectly. This dual binding hypothesis reconciles the initial docking prediction of a common competitive site with CAF's experimentally observed allosteric inhibition mechanism, underscoring the complexity of its mole-

Open Access Article. Published on 21 January 2026. Downloaded on 3/3/2026 10:07:28 AM. This article is licensed under a Creative Commons Attribution 3.0 Unported Licence.

cular recognition. In contrast, 24MCAF, despite its moderately lower binding affinity ($K_D \approx 1.76$ μM), demonstrated high enzymatic inhibitory potency, with a notably lower IC_{50} (0.04 μM) compared to CAF (0.46 μM). This reflects its role as a competitive inhibitor, effectively blocking substrate access to the catalytic site. Cell-based experiments in HepG2 cells further highlight the distinct yet complementary roles of these molecules that share a common sterol ferulate scaffold, but differ for a methylene group. CAF significantly reduces the total and free cholesterol levels by approximately 30% (comparable to simvastatin), and robustly activates the SREBP-2 signaling pathway, indicated by the increased expression of SREBP-2 (M), HMGCR and LDL receptor as a feedback response to cholesterol depletion. Conversely, 24MCAF, while inducing a moderate cholesterol reduction (~15%), elicits the most pronounced upregulation of cholesterol efflux transporter ABCG1 (3.6-fold increase) and enhances expression of ABCA1 and CYP7A1, indicative of augmented cholesterol clearance through efflux and catabolism pathways. Together, these findings reveal a nuanced interplay where CAF's strong, stable binding and allosteric modulation primarily suppress cholesterol biosynthesis, while 24MCAF's potent competitive inhibition combined with enhanced cholesterol efflux contribute synergistically to balance cellular cholesterol synthesis and secretion. This differential but complementary mode of action among γ-oryzanol constituents provides a molecular basis for the lipid-lowering effects of γ-oryzanol and highlights their therapeutic potential. Collectively, cycloartenyl ferulates emerged as promising natural molecules for cholesterol management, combining effective enzyme inhibition with stimulation of cholesterol clearance mechanisms, most importantly in a range of concentrations that exhibited safe profiles in a hepatic cell model. Likewise, other parallel *in vitro* and *in vivo* studies indicate that, at physiologically relevant concentrations, γ-oryzanol protects against oxidative stress, inflammation, and apoptosis in liver cells without inducing cytotoxicity or mitochondrial stress. Acute toxicity has been reported only at extremely high doses (>2000 mg kg^{-1} day^{-1} in rodents), with no toxicologically significant changes or histopathological abnormalities observed, including in muscle tissue, suggesting a high safety margin. Biomarkers such as ALT, AST, catalase, glutathione, and malondialdehyde consistently support a cytoprotective and antioxidant effect.[48,49] Furthermore, documented drug–drug interactions for γ-oryzanol or its major constituents are negligible, with minimal impact on CYP-mediated drug metabolism at standard doses.[50] Nevertheless, given the potential for additive or antagonistic interactions during combination therapy with other cholesterol-lowering drugs, particularly in co-treatments involving CAF and 24MCAF which target distinct HMGCR sites, caution is demanded and should be considered during clinical application. In this perspective, future studies focused on the pharmacokinetics, bioavailability, and *in vivo* efficacy of γ-oryzanol components are essential to fully evaluate their safe application as effective alternatives or adjuncts to conventional statin therapy.

Author contributions

The manuscript was written through contributions of all authors. All authors have given approval to the final version of the manuscript.

Conflicts of interest

There are no conflicts to declare.

Data availability

The data supporting this article have been included as part of the supplementary information (SI). Supplementary information is available. See DOI: https://doi.org/10.1039/d5fo03394b.

Acknowledgements

The work received support by the National Recovery and Resilience Plan (NRRP), Mission 4, Component 2, Investment 1.1, Call for tender No. 104 published on 2.2.2022 by the Italian Ministry of University and Research (MUR), funded by the European Union – NextGenerationEU – Project Title "Combined effect of gamma-oryzanol and probiotics in counteracting the hallmarks of pathological aging (ORPHEA)" – CUP 2022ZRSHHB - Grant Assignment Decree No. 1017 adopted on 7.7.2023 by the Italian Ministry of Ministry of University and Research (MUR).

References

1 H. The Lancet Digital, Promises and challenges of digital tools in cardiovascular care, *Lancet Digital Health*, 2024, **6**, e673.
2 A. L. Catapano, I. Graham, G. De Backer, O. Wiklund, M. J. Chapman, H. Drexel, A. W. Hoes, C. S. Jennings, U. Landmesser, T. R. Pedersen, Ž Reiner, G. Riccardi, M.-R. Taskinen, L. Tokgozoglu, W. M. M. Verschuren, C. Vlachopoulos, D. A. Wood and J. L. Zamorano, 2016 ESC/EAS Guidelines for the Management of Dyslipidaemias, *Eur. Heart J.*, 2016, **37**, 2999–3058.
3 R. Collins, C. Reith, J. Emberson, J. Armitage, C. Baigent, L. Blackwell, R. Blumenthal, J. Danesh, G. D. Smith, D. DeMets, S. Evans, M. Law, S. MacMahon, S. Martin, B. Neal, N. Poulter, D. Preiss, P. Ridker, I. Roberts, A. Rodgers, P. Sandercock, K. Schulz, P. Sever, J. Simes, L. Smeeth, N. Wald, S. Yusuf and R. Peto, Interpretation of the evidence for the efficacy and safety of statin therapy, *Lancet*, 2016, **388**, 2532–2561.
4 F. Mach, C. Baigent, A. L. Catapano, K. C. Koskinas, M. Casula, L. Badimon, M. J. Chapman, G. G. De Backer, V. Delgado, B. A. Ference, I. M. Graham, A. Halliday,

 This journal is © The Royal Society of Chemistry 2026

Open Access Article. Published on 21 January 2026. Downloaded on 3/3/2026 10:07:28 AM. This article is licensed under a Creative Commons Attribution 3.0 Unported Licence.

U. Landmesser, B. Mihaylova, T. R. Pedersen, G. Riccardi, D. J. Richter, M. S. Sabatine, M.-R. Taskinen, L. Tokgozoglu, O. Wiklund and E. S. D. Group, 2019 ESC/EAS Guidelines for the management of dyslipidaemias: lipid modification to reduce cardiovascular risk: The Task Force for the management of dyslipidaemias of the European Society of Cardiology (ESC) and European Atherosclerosis Society (EAS), *European Heart Journal*, 2019, **41**, 111–188.

5 H. Naci, J. Brugts and T. Ades, Comparative tolerability and harms of individual statins: a study-level network meta-analysis of 246 955 participants from 135 randomized, controlled trials, *Circ. Cardiovasc. Qual. Outcomes*, 2013, **6**, 390–399.

6 M. Cuccioloni, M. Mozzicafreddo, M. Spina, C. N. Tran, M. Falconi, A. M. Eleuteri and M. Angeletti, Epigallocatechin-3-gallate potently inhibits the in vitro activity of hydroxy-3-methyl-glutaryl-CoA reductase, *J. Lipid Res.*, 2011, **52**, 897–907.

7 A. Mahdavi, M. Bagherniya, O. Fakheran, Ž Reiner, S. Xu and A. Sahebkar, Medicinal plants and bioactive natural compounds as inhibitors ofHMG–CoAreductase: A literature review, *BioFactors*, 2020, **46**, 906–926.

8 M. J. Lerma-García, J. M. Herrero-Martínez, E. F. Simó-Alfonso, C. R. B. Mendonça and G. Ramis-Ramos, Composition, industrial processing and applications of rice bran γ-oryzanol, *Food Chem.*, 2009, **115**, 389–404.

9 S. Eady, A. Wallace, J. Willis, R. Scott and C. Frampton, Consumption of a plant sterol-based spread derived from rice bran oil is effective at reducing plasma lipid levels in mildly hypercholesterolaemic individuals, *Br. J. Nutr.*, 2011, **105**, 1808–1818.

10 C.-W. Chen and H.-H. Cheng, A Rice Bran Oil Diet Increases LDL-Receptor and HMG-CoA Reductase mRNA Expressions and Insulin Sensitivity in Rats with Streptozotocin/Nicotinamide-Induced Type 2 Diabetes, *J. Nutr.*, 2006, **136**, 1472–1476.

11 F. Mas'ud, H. Bangngalino, M. Yusuf, S. Suhardi and M. Sayuti, Rice bran oil extraction by ethanol: optimization of γ-oryzanol and polyphenol, *Food Res.*, 2023, **7**, 289–296.

12 R. Heidtmann-Bemvenuti, N. S. Nora and E. Badiale-Furlong, Extraction of γ-oryzanol from rice bran, *Cienc. Agrotecnol.*, 2012, **36**, 665–673.

13 R. A. Nugrahani, T. Y. Hendrawati, U. H. Hasyim, F. Sari and A. I. Ramadhan, Kinetic parameter for scale-up and γ-oryzanol content of rice bran oil as antioxidant: Comparison of maceration, ultrasonication, pneumatic press extraction, *Heliyon*, 2024, **10**, e30880.

14 A. Kayathi, P. P. Chakrabarti, L. Bonfim-Rocha, L. Cardozo-Filho, A. Bollampalli and V. Jegatheesan, Extraction of γ-Oryzanol from defatted rice bran using supercritical carbon dioxide (SC-CO2): Process optimisation of extract yield, scale-up and economic analysis, *Process Saf. Environ. Prot.*, 2021, **148**, 179–188.

15 J. P. Baixinho, M. Cardeira, A. Bento-Silva, A. M. C. Partidário, A. T. Serra, M. D. R. Bronze and N. Fernández, Optimization of Supercritical Fluid Extraction for the Recovery of γ-Oryzanol-Rich Extracts with Improved Bioactivity from Rice Bran, *Antioxidants*, 2025, **14**, 206–220.

16 C. Lemus, A. Angelis, M. Halabalaki and A. L. Skaltsounis, in *Wheat and Rice in Disease Prevention and Health*, 2014, pp. 409–430, DOI: 10.1016/b978-0-12-401716-0.00032-5.

17 H. Juricic, M. Cuccioloni, L. Bonfili, M. Angeletti, D. Uberti, A. M. Eleuteri, G. Abate and V. Cecarini, Biochemical, Biological, and Clinical Properties of γ-Oryzanol, *Antioxidants*, 2025, **14**, 1099–1117.

18 A. Mastinu, S. A. Bonini, W. Rungratanawanich, F. Aria, M. Marziano, G. Maccarinelli, G. Abate, M. Premoli, M. Memo and D. Uberti, Gamma-oryzanol Prevents LPS-induced Brain Inflammation and Cognitive Impairment in Adult Mice, *Nutrients*, 2019, **11**, 728–740.

19 C. E. Cabral and M. R. S. T. Klein, Phytosterols in the Treatment of Hypercholesterolemia and Prevention of Cardiovascular Diseases, *Arq. Bras. Cardiol.*, 2017, **109**, 475–482.

20 F. Barkas, E. Bathrellou, T. Nomikos, D. Panagiotakos, E. Liberopoulos and M. D. Kontogianni, Plant Sterols and Plant Stanols in Cholesterol Management and Cardiovascular Prevention, *Nutrients*, 2023, **15**, 2845–2860.

21 A. F. G. Cicero and A. Gaddi, Rice Bran Oil and γ–Oryzanol in the Treatment of Hyperlipoproteinaemias and Other Conditions, *Phytother. Res.*, 2001, **15**, 277–289.

22 A. Berger, D. Rein, A. Schäfer, I. Monnard, G. Gremaud, P. Lambelet and C. Bertoli, Similar cholesterol-lowering properties of rice bran oil, with varied γ-oryzanol, in mildly hypercholesterolemic men, *Eur. J. Nutr.*, 2004, **44**, 163–173.

23 J. Luo, H. Yang and B.-L. Song, Mechanisms and regulation of cholesterol homeostasis, *Nat. Rev. Mol. Cell Biol.*, 2019, **21**, 225–245.

24 B. B. Madison, Srebp2: A master regulator of sterol and fatty acid synthesis, *J. Lipid Res.*, 2016, **57**, 333–335.

25 M. C. Phillips, Molecular Mechanisms of Cellular Cholesterol Efflux, *J. Biol. Chem.*, 2014, **289**, 24020–24029.

26 J. Umar, E. Suyanto, T. A. Wihastuti and F. Fatchiyah, Virtual selection of γ-oryzanol derivatives of brown rice (Oryza sativa L.) blocking HMG-CoA reductase in hypercholesterolemia disease, *Berk. Penelit. Hayati*, 2025, **31**, 19–27.

27 E. S. Istvan, M. Palnitkar, S. K. Buchanan and J. Deisenhofer, Crystal structure of the catalytic portion of human HMG-CoA reductase: insights into regulation of activity and catalysis, *EMBO J.*, 2000, **19**, 819–830.

28 H. Prinz, Hill coefficients, dose–response curves and allosteric mechanisms, *J. Chem. Biol.*, 2009, **3**, 37–44.

29 A. Endo, The discovery and development of HMG-CoA reductase inhibitors, *J. Lipid Res.*, 1992, **33**, 1569–1582.

30 J. L. Goldstein and M. S. Brown, Regulation of the mevalonate pathway, *Nature*, 1990, **343**, 425–430.

31 H. Shimano, Sterol regulatory element-binding proteins (SREBPs): transcriptional regulators of lipid synthetic genes, *Prog. Lipid Res.*, 2001, **40**, 439–452.

Open Access Article. Published on 21 January 2026. Downloaded on 3/3/2026 10:07:28 AM. This article is licensed under a Creative Commons Attribution 3.0 Unported Licence.

32 T. Daya, A. Breytenbach, L. Gu and M. Kaur, Cholesterol metabolism in pancreatic cancer and associated therapeutic strategies, *Biochim. Biophys. Acta, Mol. Cell Biol. Lipids*, 2025, **1870**, 159578–159592.
33 P. Parini, U. Gustafsson, M. A. Davis, L. Larsson, C. Einarsson, M. Wilson, M. Rudling, H. Tomoda, S. Omura, S. Sahlin, B. Angelin, L. L. Rudel and M. Eriksson, Cholesterol Synthesis Inhibition Elicits an Integrated Molecular Response in Human Livers Including Decreased ACAT2, *Arterioscler., Thromb., Vasc. Biol.*, 2008, **28**, 1200–1206.
34 Y.-J. Choi, S. J. Lee, H. I. Kim, H. J. Lee, S. J. Kang, T. Y. Kim, C. Cheon and S.-G. Ko, Platycodin D enhances LDLR expression and LDL uptake via down-regulation of IDOL mRNA in hepatic cells, *Sci. Rep.*, 2020, **10**, 19834–19855.
35 J. V. F. Echenique, G. Alvarez-Rivera, V. M. A. Luna, A. F. V. da Cruz Antonio, M. R. Mazalli, E. Ibañez, A. Cifuentes and A. L. de Oliveira, Pressurized liquid extraction with ethanol in an intermittent process for rice bran oil: Evaluation of process variables on the content of β-sitosterol and phenolic compounds, antioxidant capacity, acetylcholinesterase inhibitory activity, and oil quality, *LWT*, 2024, **207**, 116650–116658.
36 G. Abate, A. Pezzotta, M. Pucci, V. Bortolotto, G. Ribaudo, S. A. Bonini, A. Mastinu, G. Maccarinelli, A. Ongaro, E. Tirelli, D. Zizioli, A. Gianoncelli, M. Memo, M. Grilli and D. Uberti, The Bioactive Gamma-Oryzanol from Oryza sativa L. Promotes Neuronal Differentiation in Different In Vitro and In Vivo Models, *Antioxidants*, 2024, **13**, 969–983.
37 I. N. Papadoyannis and H. G. Gika, Peak Purity Determination with a Diode Array Detector, *J. Liq. Chromatogr. Relat. Technol.*, 2007, **27**, 1083–1092.
38 G. M. Morris, R. Huey, W. Lindstrom, M. F. Sanner, R. K. Belew, D. S. Goodsell and A. J. Olson, AutoDock4 and AutoDockTools4: Automated docking with selective receptor flexibility, *J. Comput. Chem.*, 2009, **30**, 2785–2791.
39 R. W. Sarver, E. Bills, G. Bolton, L. D. Bratton, N. L. Caspers, J. B. Dunbar, M. S. Harris, R. H. Hutchings, R. M. Kennedy, S. D. Larsen, A. Pavlovsky, J. A. Pfefferkorn and G. Bainbridge, Thermodynamic and Structure Guided Design of Statin Based Inhibitors of 3-Hydroxy-3-Methylglutaryl Coenzyme A Reductase, *J. Med. Chem.*, 2008, **51**, 3804–3813.
40 H. M. Berman, The Protein Data Bank, *Nucleic Acids Res.*, 2000, **28**, 235–242.
41 S. Kim, J. Chen, T. Cheng, A. Gindulyte, J. He, S. He, Q. Li, B. A. Shoemaker, P. A. Thiessen, B. Yu, L. Zaslavsky, J. Zhang and E. E. Bolton, PubChem 2023 update, *Nucleic Acids Res.*, 2023, **51**, D1373–D1380.
42 M. D. Hanwell, D. E. Curtis, D. C. Lonie, T. Vandermeersch, E. Zurek and G. R. Hutchison, Avogadro: an advanced semantic chemical editor, visualization, and analysis platform, *J. Cheminf.*, 2012, **4**, 17.
43 V. Cecarini, M. Cuccioloni, C. Gong, Z. Liu, L. Bonfili, M. Angeletti, S. Angeloni, L. Alessandroni, G. Sagratini, H. Liu and A. M. Eleuteri, Role of Panax ginseng and ginsenosides in regulating cholesterol homeostasis, *Food Biosci.*, 2023, **56**, 103256–103264.
44 P. R. Edwards, P. A. Lowe and R. J. Leatherbarrow, Ligand loading at the surface of an optical biosensor and its effect upon the kinetics of protein–protein interactions, *J. Mol. Recognit.*, 1997, **10**, 128–134.
45 M. Cuccioloni, L. Bonfili, V. Cecarini, M. Nabissi, R. Pettinari, F. Marchetti, R. Petrelli, L. Cappellacci, M. Angeletti and A. M. Eleuteri, Exploring the Molecular Mechanisms Underlying the in vitro Anticancer Effects of Multitarget–Directed Hydrazone Ruthenium(II)–Arene Complexes, *ChemMedChem*, 2019, **15**, 105–113.
46 E. S. Istvan and J. Deisenhofer, Structural mechanism for statin inhibition of HMG-CoA reductase, *Science*, 2001, **292**, 1160–1164.
47 M. M. Bradford, A rapid and sensitive method for the quantitation of microgram quantities of protein utilizing the principle of protein-dye binding, *Anal. Biochem.*, 1976, **72**, 248–254.
48 G. Shu, Y. Qiu, J. Hao, Q. Fu and X. Deng, γ-Oryzanol alleviates acetaminophen-induced liver injury: roles of modulating AMPK/GSK3β/Nrf2 and NF-κB signaling pathways, *Food Funct.*, 2019, **10**, 6858–6872.
49 S.-H. Moon, D. Kim, N. Shimizu, T. Okada, S. Hitoe and H. Shimoda, Ninety-day oral toxicity study of rice-derived γ-oryzanol in Sprague-Dawley rats, *Toxicol. Rep.*, 2017, **4**, 9–18.
50 K. Umehara, Y. Shimokawa and G. Miyamoto, Effect of GAMMA-Oryzanol on Cytochrome P450 Activities in Human Liver Microsomes, *Biol. Pharm. Bull.*, 2004, **27**, 1151–1153.

This journal is © The Royal Society of Chemistry 2026